Reversing the perturbation in nonequilibrium molecular dynamics: An easy way to calculate the shear viscosity of fluids

Florian Müller-Plathe
Max-Planck-Institut für Polymerforschung, Ackermannweg 10, D-55128 Mainz, Germany
(Received 2 November 1998)

A nonequilibrium method for calculating the shear viscosity is presented. It reverses the cause-and-effect picture customarily used in nonequilibrium molecular dynamics: the effect, the momentum flux or stress, is imposed, whereas the cause, the velocity gradient or shear rate, is obtained from the simulation. It differs from other Norton-ensemble methods by the way in which the steady-state momentum flux is maintained. This method involves a simple exchange of particle momenta, which is easy to implement. Moreover, it can be made to conserve the total energy as well as the total linear momentum, so no coupling to an external temperature bath is needed. The resulting raw data, the velocity profile, is a robust and rapidly converging property. The method is tested on the Lennard-Jones fluid near its triple point. It yields a viscosity of 3.2-3.3, in Lennard-Jones reduced units, in agreement with literature results. [S1063-651X(99)03105-0]

PACS number(s): 66.20.+d, 61.20.Ja, 02.70.−c

I. INTRODUCTION

Linear-response theory relates a flux J (e.g., matter, energy, momentum) to a thermodynamic driving force or field E, which usually is a gradient of some quantity (e.g., activity, temperature, flow velocity). The proportionality constant is the corresponding transport coefficient κ:

$$J = -\kappa E. \tag{1}$$

The flux is defined as the amount of the quantity transported per time through an area perpendicular to the flux direction. We note that, e.g., in an anisotropic medium, the directions of J and E need not be collinear in which case their vectorial nature has to be taken into consideration and κ becomes a tensor. In isotropic fluids, however, we can use the scalar form [Eq. (1)].

Transport coefficients can be calculated by equilibrium molecular dynamics (MD) calculations using the appropriate Einstein or Green-Kubo relations [1–3]. The alternative route are nonequilibrium molecular dynamics (NEMD) simulations [3,4]: An appropriate perturbation E is applied which is not necessarily the same as in the experiment, but which can be shown to generate the same response [4]. Then, the ensemble average of the resulting flux $\langle J \rangle$ is measured and the ratio of flux and field gives the transport coefficient κ. There are many ways of setting up NEMD simulations [4]. In most of them, the field is applied and the flux is measured.

In this contribution, we consider a scheme in which cause and effect are reversed in an NEMD simulation: The flux is imposed and the corresponding field is measured. Such methods, also known as Norton-ensemble methods [4–7], have their advantages in cases where the flux is difficult to define microscopically or is slowly converging. In contrast to previous methods, the one presented in this article can be made, in certain cases, to conserve the total energy as well as the total linear momentum, so it can be used in a microcanonical ensemble, i.e., without an additional thermostat. Moreover, it is simple to implement and generates intermediate data which is robust and easy to analyse. Similar concepts have been used by Hafskjold *et al.* [8–10] and by us [11–13] to calculate thermal conductivities and Soret coefficients. In this article, it is extended to the practically more important calculation of the shear viscosity.

II. METHOD

The shear viscosity connects a shear field with a flux of transverse linear momentum [14]. The shear field is a gradient of one component of the fluid velocity, say the x direction, with respect to another direction, say the z direction, $\partial v_x / \partial z$. It is also denoted as the shear rate. The momentum flux $j_z(p_x)$ is collinear: It is the x component of the momentum p_x transported in z direction per given time and per unit area, see Fig. 1. It can also be regarded as an off-diagonal (xz) component of the stress tensor. The proportionality coefficient is the shear viscosity η:

$$j_z(p_x) = -\eta \frac{\partial v_x}{\partial z}. \tag{2}$$

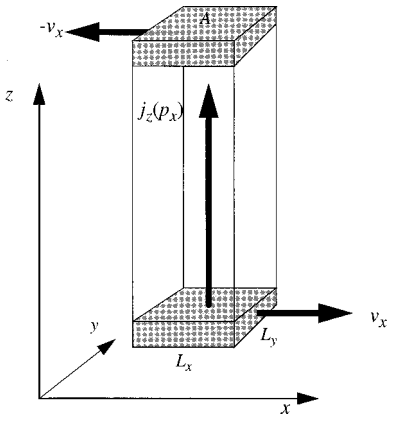

FIG. 1. Geometry of the nonequilibrium situation. A gradient in v_x is set up in the z direction by shearing the liquid. As a result, x momentum flows in the z direction, giving rise to a momentum flux $j_z(p_x)$ through the xy plane of area A.

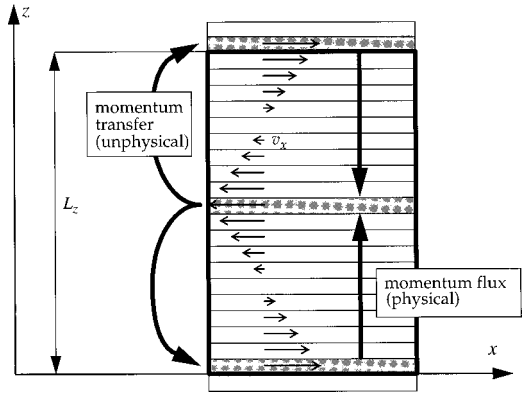

FIG. 2. Schematic view of the periodic simulation box.

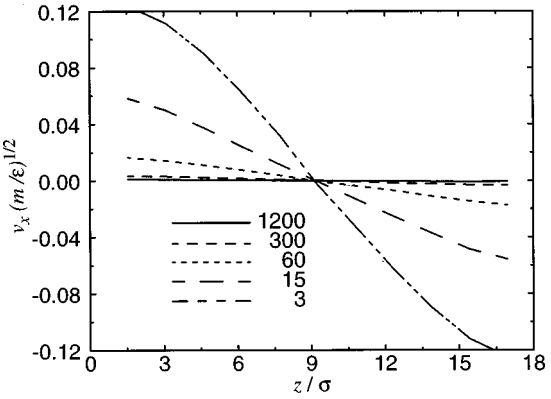

FIG. 3. Velocity profiles in the simulation cell (only one-half is shown) for different intervals of momentum interchange (number of time steps W between momentum exchanges). Lennard-Jones reduced units are used.

The momentum flux $j_z(p_x)$ is defined as the momentum flowing through a surface perpendicular to the flux direction (z) of area A during a time t. In SI units it has, therefore, the dimension $\mathrm{kg\,m^{-1}\,s^{-2}}$. Since the velocity gradient has the unit $\mathrm{s^{-1}}$, the unit of the viscosity is $1\,\mathrm{Poise}=1\,\mathrm{kg\,m^{-1}\,s^{-1}}$.

The momentum flux is imposed on the system in an unphysical way. The periodic simulation box is subdivided into slabs along the z coordinate (Fig. 2). The atoms inside the slab at $z=0$ (and its period images) are propelled in the $+x$ direction, those inside the slab at $z=L_z/2$ (with L_z the box length in the z direction) in the $-x$ direction. This is accomplished by finding the atom most moving against the desired slab movement: In the slab moving in the $+x$ direction ($z=0$), the atom with the largest momentum component in the $-x$ direction (=the atom with the smallest p_x) is found. Likewise, in the slab moving in the $-x$ direction ($z=L_z/2$), the atom with the largest momentum component in the $+x$ direction (=the atom with the largest p_x) is found. Then the p_x of the two atoms are interchanged. N.B. If both atoms have the same mass, the unphysical momentum swap conserves both linear momentum and kinetic energy of the system as a whole. Since atom positions are not changed, the potential energy and, hence, the total energy of the system is conserved.

The amount of momentum Δp_x transferred from the $z=L_z/2$ slab to the $z=0$ slab is precisely known. If momentum swaps are repeated periodically, the total momentum transferred in a simulation P_x is the sum of the Δp_x. The system responds to the nonequilibrium situation by letting momentum flow in the opposite direction via a physical mechanism (friction). In the steady state, the rate of momentum transferred unphysically by momentum swaps is equal to that of momentum flowing back through the fluid by friction. Hence, the momentum flux $j_z(p_x)$ can be calculated.

$$j(p_x)=\frac{P_x}{2tA}, \tag{3}$$

where t is the length of the simulation and $A=L_xL_y$ (Fig. 1), the factor 2 arises because of the periodicity of the system [11].

The physical momentum current gives rise to a velocity profile in the fluid (see Fig. 2). The flow velocity v_x in x direction in every slab is calculated as the average of the $v_{x,i}$ of all atoms i in that slab. If the momentum flux is not too large the velocity profile is approximately linear and $\langle \partial v_x/\partial z\rangle$ and its error can be obtained by a linear regression. The viscosity is then given by Eq. (2). Its error can be estimated using the rules for error propagation from the error in the velocity gradient, the value for $j_z(p_x)$ at steady state being known exactly. If the velocity profile is not linear this means that the efficiency of the momentum transfer ($\sim 1/\eta$) is not uniform across the system. This indicates that the momentum flux is too large, that the mechanism of momentum transfer is no longer uniform, and that the linear-response regime has been left. Velocity profiles are shown in Fig. 3. The interval between velocity exchanges W is varied between 3 and 1200 time steps. The applied momentum flux thus varies by more than 2 orders of magnitude. Except for the highest momentum fluxes ($W\leqslant 15\Delta t$), the velocity gradient is uniform throughout the system. Surprisingly, even in the slightly nonlinear regime the viscosity can be calculated with reasonable accuracy (see below).

At this point, one might ask how there can be shear flow apparently without viscous heating. The answer is that there is viscous heating but the excess heat is drained by the momentum exchange itself. It acts as an internal thermostat, i.e., a mechanism that removes the heat generated by friction. The algorithm, that maybe thought of as a Maxwell demon, selectively picks particles with the largest velocity component $\mathbf{u}_i=\mathbf{v}_i-\langle\mathbf{v}\rangle$ against the flow direction of the slab $\langle\mathbf{v}\rangle$. The peculiar velocities $\mathbf{u}_i$, on the other hand, define the slab temperature. After the exchange, the peculiar velocity of the particle is in the direction of the local flow and, although the absolute velocity is on average unchanged, the peculiar velocity and, thus, the temperature has decreased. Therefore, the two slabs in which the momentum exchange takes place are the heat sinks where the heat generated by friction is disposed of. As a consequence, a temperature profile across the box is expected. This is indeed found in Fig. 4, where we show the fraction of kinetic energy calculated from the peculiar velocities, i.e., our definition of local temperature. For the strongest perturbations [$W=3$,15, Fig. 4(b)] the temperature profile is a parabola. This is intuitively understood, since a linear flow velocity profile causes a quadratic kinetic energy profile associated with the flow. For the small perturbations [Fig. 4(a)], the situation is less clear. There, the regions of strongest viscous heating are not necessarily halfway be-

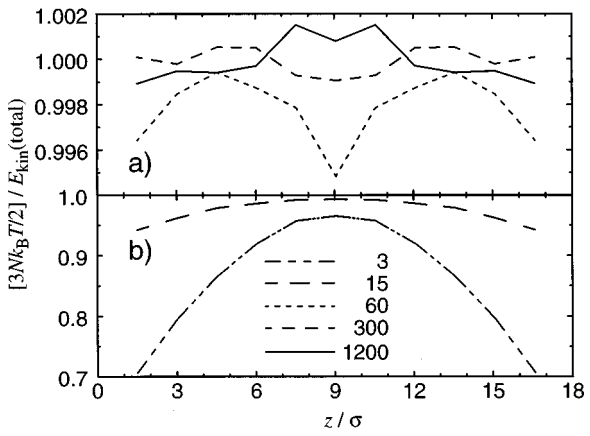

FIG. 4. Temperature profile across the simulation cell. For each slab, the figure shows the kinetic energy calculated from peculiar velocities, i.e., the ''temperature,'' relative to the total kinetic energy calculated from the total velocities, i.e., including the drift velocity. In order to improve statistics, temperatures of symmetrically equivalent slabs have been averaged. The root-mean-square fluctuations of temperatures within individual slabs are of the order of 0.1 on the scale of this figure. For clarity, the figure is split into two parts with different scaling of the ordinate. Lennard-Jones reduced units are used.

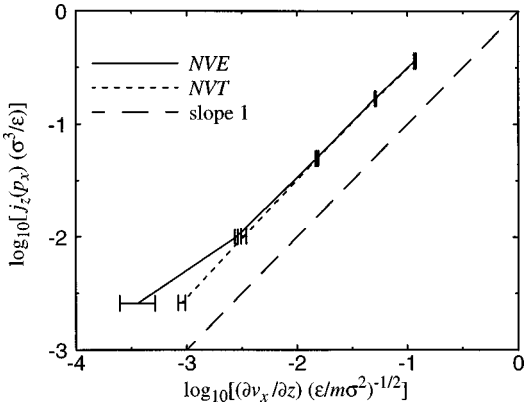

FIG. 5. Linear response relation between the velocity gradient (shear rate) and the momentum flux (stress). The plot follows the customary presentation with the perturbation as the abscissa and the resulting flux as the ordinate, although the perturbation is applied reversely in this work. Solid line, constant energy; dashed line, constant temperature. Lennard-Jones reduced units are used.

tween the heat sinks. For the time being, we report this as a phenomenon. It still remains to be clarified if this is a physical effect or results from insufficient statistics or from the finite width of the slabs.

III. COMPUTATIONAL DETAILS

The system was composed of 2592 atoms of mass m interacting via the Lennard-Jones (LJ) potential

$$V(r)=4\varepsilon\left[\left(\frac{\sigma}{r}\right)^{12}-\left(\frac{\sigma}{r}\right)^{6}\right] \tag{4}$$

with a cutoff of 3σ. The size of the orthorhombic periodic simulation cell was $10.0587\sigma\times10.0587\sigma\times30.1762\sigma$, corresponding to a reduced number density $\rho^*=\rho\sigma^3=0.849$. The temperature was $T^*=k_BT/\varepsilon=0.722$. The system was thus very close to the triple point of the LJ fluid. In the constant-T runs, the temperature was maintained by weakly coupling to a temperature bath [15] with the coupling time τ^* of $0.464(\varepsilon/m\sigma^2)^{1/2}$, unless noted otherwise. Constant-energy runs were preceded by equilibration runs at the same temperature. The time step was $\Delta t^*=\Delta t(\varepsilon/m\sigma^2)^{1/2}=6.965\times10^{-3}$. A multiple-time-step scheme based on the velocity-Verlet algorithm [16] was used with the parameters as in Ref. [11]. A Verlet neighbor list was updated every 12 time steps, the update used indexing of the particles according to their z direction [11]. The momentum flux was imposed in the z direction, the number of slabs was 20 (see Fig. 2). The simulation times were 15 000 time steps ($W=3$), 60 000 time steps ($W=15,60$), and 300 000 time steps ($W=300,1200$), respectively. For reference, the LJ reduced units of the relevant transport quantities are $j_z^*(p_x)=j_z(p_x)\sigma^3\varepsilon^{-1}$, $(\partial v_x/\partial z)^*=(\partial v_x/\partial z)(m\sigma^2/\varepsilon)^{1/2}$, $\eta^*=\eta\sigma^2(\varepsilon m)^{-1/2}$.

The momentum-exchange algorithm is, in principle, energy-conserving. However, there is a small nonconservation of energy in practice due to discretizing Newton's equation of motion into finite time steps. The Verlet algorithm tacitly assumes that, over the length of the time step, the force acting on a particle is constant. This is no longer true if a discontinuity is imposed on the trajectory and it will lead to some loss of accuracy in the integration. In practical calculations of viscosities, the perturbation can be considered small, since only two out of several thousand particles are affected every several dozen or several hundred time steps. Moreover, in our analysis of the velocity profile we disregard the two slabs in which the momentum exchange takes place. On the other hand, the discontinuous trajectories make the algorithm difficult to analyze from a purely theoretical point of view. One also has to keep in mind that the momentum exchange algorithm produces not only the intended velocity profile of periodicity L_z, but also a concomitant temperature profile of periodicity $L_z/2$.

IV. RESULTS AND DISCUSSION

The validity of the linear-response relation [Eq. (2)] is tested in Fig. 5. Linear response appears to hold even for the strongest applied perturbation. This indicates that, although the viscosity is not completely uniform over the simulation cell (see Fig. 3), these heterogeneities tend to cancel out. At very small momentum transfer, the resulting velocity gradient is blurred by noise, so longer simulation times would be needed here. Constant-temperature and constant-energy simulations are both linear and give the same slope in regions were the slope converges well.

For all perturbations, the viscosity has been calculated via Eq. (2). In Fig. 6, it is seen that the viscosity is not well defined at very low perturbations ($W=300,1200$). At the strongest perturbation ($W=3$), the onset of nonlinearity is visible. In between ($W=15,60$), there is a usefully wide plateau region (the abscissa in Fig. 6 is plotted logarithmically) from which the viscosity can be reliably obtained. Except for the two smallest perturbations, constant-energy and constant-temperature simulations give the same viscosity. Most calcu-

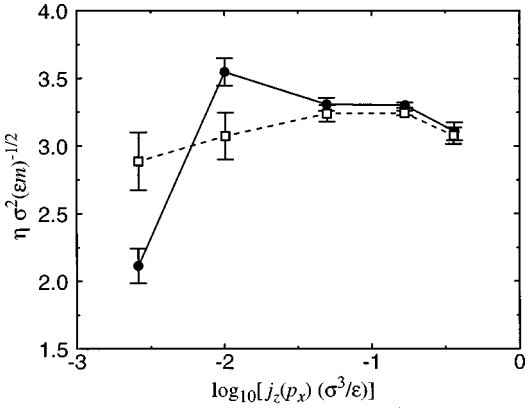

FIG. 6. Lennard-Jones triple-point viscosity calculated at different momentum transfer rates. Solid circles, constant energy; open squares, constant temperature. Lennard-Jones reduced units are used.

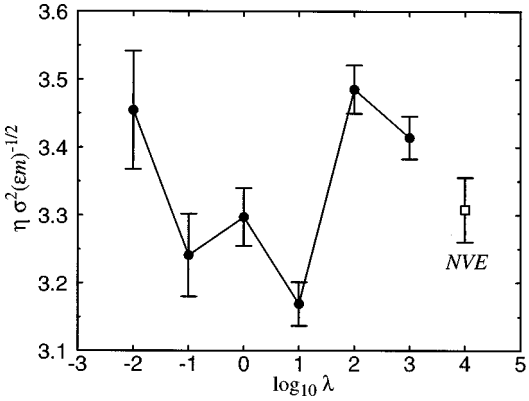

FIG. 7. Influence of the coupling time of the weak-coupling thermostat on the calculated viscosity. The coupling time τ^* is $\lambda \times 0.464(\varepsilon/m\sigma^2)^{1/2}$, the logarithm of the scale factor λ is used as the abscissa. The momentum-exchange interval W was 60 for all calculations in this figure. Lennard-Jones reduced units are used.

lations of the LJ triple-point viscosity have used considerably smaller systems (108 to 256 particles) which yield a η^* of about 3.0. However, using larger systems (up to 1372 particles), Palmer [17] has estimated $\eta^*(k^*=0)$ to be 3.25 ± 0.08, $k^*=k\sigma$ being the reciprocal lattice vector. Our simulation cell is large enough in the z direction for k^* to be close to zero. Therefore, it is no surprise that all our plateau values of $\eta^*=3.2$-3.3 are very close to the literature estimate. Note, however, that because of the periodicity of our perturbation, the viscosity calculated by this method belongs to a certain k, and the $k^*=0$ limit has to be found by systematically varying the box length.

The nonequilibrium scheme presented above conserves total linear momentum as well as the total energy of the system. Hence, it does not require an external thermostat. On the other hand, one may want to use it together with a thermostat (and/or manostat) for practical reasons. It is, therefore, worth knowing if and how a thermostat affects the value of the calculated viscosity. The Berendsen thermostat [15] is often used for its simplicity and robustness, even though it is not derived from a Hamiltonian and has not been shown to generate a canonical ensemble. In Fig. 7 it is investigated how the intensity of thermostatting, the value of the coupling time τ^*, changes the calculated viscosity. To this end, τ^* has been varied over 6 orders of magnitude. Figure 7 shows that the viscosity does depend on the choice of τ^*. This dependence appears to be rather erratic. All of the values are, however, close to each other, the standard deviation being 0.12, and to the microcanonical value. Therefore, thermostats have to be watched for their influence on the viscosity if used with this algorithm, as with others, but they are not likely to distort the results qualitatively.

V. SUMMARY AND OUTLOOK

The nonequilibrium method for calculating the shear viscosity presented reverses the customary cause-and-effect picture: the effect, the momentum flux, is imposed, whereas the cause, the velocity gradient, is calculated from the simulation. It differs from other Norton-ensemble methods by the way, in which the steady-state momentum flux is maintained. It involves a simple exchange of particle momenta, which is easy to implement. The exchange events, although unphysical, conserve the total linear momentum as well as the total energy if the masses of the particles are equal. In this case, no external thermostat is needed. The resulting raw data, the velocity profile, is a robust and rapidly converging property.

A similar momentum and energy-conserving reverse-perturbation scheme has recently been used to study thermal conductivity and thermal diffusion [11–13]. There, the relevant energy flux could also be set up using only velocity exchanges between particles. It is easy to see how the principle of reverse perturbation can be extended to calculate other transport coefficients. However, it is less clear if an extension is useful in all cases. For example, it would be nice to calculate the mutual diffusion coefficient in a binary fluid. In order to maintain an interdiffusion current, one would have to exchange particle identities, which means exchanging force field parameters. While this is possible, it necessarily destroys the conservation of total energy, which is the beauty of the present method. Of course, one may give both species the same interaction parameters and just ''color'' (label) them differently. This is an established method for calculating the self-diffusion coefficient [18] which is obtained from the color gradient.

ACKNOWLEDGMENTS

I would like to thank Professor Denis J. Evans who contributed much to my understanding of the algorithm, and Dr. Burkhard Dünweg for many enlightening discussions about the subject.

[1] M. P. Allen and D. J. Tildesley, *Computer Simulation of Liquids* (Oxford Science, Oxford, 1987).
[2] D. A. McQuarrie, *Statistical Mechanics* (Harper Collins, New York, 1976).
[3] R. Kubo, M. Toda, and N. Hashitsume, *Statistical Physics II* (Springer, Berlin, 1985).
[4] D. J. Evans and G. P. Morriss, *Statistical Mechanics of Nonequilibrium Liquids* (Academic, London, 1990).
[5] D. Brown and J. H. R. Clarke, Phys. Rev. A **34**, 2093 (1986).
[6] D. J. Evans and J. F. Ely, Mol. Phys. **59**, 1043 (1986).
[7] L. J. Hood, D. J. Evans, and G. P. Morriss, Mol. Phys. **62**, 419 (1987).
[8] B. Hafskjold, T. Ikeshoji, and S. Ratkje, Mol. Phys. **80**, 1389 (1993).
[9] B. Hafskjold and T. Ikeshoji, Mol. Phys. **81**, 251 (1994).
[10] B. Hafskjold and S. Ratkje, J. Stat. Phys. **78**, 463 (1995).
[11] F. Müller-Plathe, J. Chem. Phys. **106**, 6082 (1997).
[12] D. Reith, M.Sc. thesis, University of Mainz, 1998 (unpublished).
[13] D. Reith and F. Müller-Plathe, Comput. Theor. Polym. Sci. (to be published).
[14] P. W. Atkins, *Physical Chemistry*, 5th ed. (Oxford University Press, Oxford, 1994).
[15] H. J. C. Berendsen, J. P. M. Postma, W. F. van Gunsteren, A. DiNola, and J. R. Haak, J. Chem. Phys. **81**, 3684 (1984).
[16] M. E. Tuckerman, B. J. Berne, and G. J. Martyna, J. Chem. Phys. **94**, 6811 (1991).
[17] B. J. Palmer, Phys. Rev. E **49**, 359 (1986).
[18] J. J. Erpenbeck and W. W. Wood, in *Statistical Mechanics B, Modern Theoretical Chemistry*, edited by B. J. Berne (Plenum, New York, 1977), p. 1.